INTERNATIONAL JOURNAL FOR NUMERICAL METHODS IN FLUIDS, VOL. 6, 129–154 (1986)

AN EVALUATION OF EIGHT DISCRETIZATION SCHEMES FOR TWO-DIMENSIONAL CONVECTION-DIFFUSION EQUATIONS

M. K. PATEL AND N. C. MARKATOS

Faculty of Technology, Centre for Numerical Modelling and Process Analysis, Thames Polytechnic, London SE18 6PF, U.K.

SUMMARY

A comparative study of eight discretization schemes for the equations describing convection-diffusion transport phenomena is presented. The (differencing) schemes considered are the conventional central, upwind and hybrid difference schemes,[1,2] together with the quadratic upstream,[3,4] quadratic upstream extended[4] and quadratic upstream extended revised difference[4] schemes. Also tested are the so called locally exact difference scheme[5] and the power difference scheme.[6] In multi-dimensional problems errors arise from 'false diffusion' and function approximations. It is asserted that false diffusion is essentially a multi-dimensional source of error. Hence errors associated with false diffusion may be investigated only via two- and three-dimensional problems. The above schemes have been tested for both one- and two-dimensional flows with sources, to distinguish between 'discretization' errors and 'false diffusion' errors.[7] The one-dimensional study is reported in Reference 7. For 2D flows, the quadratic upstream difference schemes are shown to be superior in accuracy to the others at all Peclet numbers, for the test cases considered. The stability of the schemes and their CPU time requirements are also discussed.

1. INTRODUCTION

The simulation of fluid-flow and heat/mass-transfer phenomena requires the numerical solution of the Navier–Stokes, energy- and species-conservation equations. These solutions involve the use of interpolation assumptions, for the variation of the fluid properties and their gradients between discrete points on a computational 'grid', that covers the domain of interest.[7] The fineness of the grid and/or the accuracy of the interpolation assumptions dictate to a large extent the accuracy of the solution. For multi-dimensional, multi-phase flow phenomena, involving 2 and 3 space dimensions and two or more sets of equations,[8–10] the power of even present day computer capacity and speed generally still proves to be the limiting factor in the use of very fine grids. Therefore, interpolation schemes are required that are sufficiently accurate to permit the performance of complex calculations with relatively coarse grids.[7] The purpose of this work is to test several of the available schemes with a view to evaluating their relative accuracy *vis-à-vis* their generality, stability and computer requirements. Two standard, well-documented, laminar flows were chosen for this test, and the schemes were tested for stability under normal, extreme and even hypothetical flow conditions (e.g. very high Reynolds number 'laminar' flow).

The schemes tested are the central difference scheme (CDS), the upwind difference scheme (UDS), the hybrid difference scheme (HDS), the quadratic upstream, quadratic upstream extended and quadratic upstream extended revised difference schemes (QUDS, QUDSE, QUDSER as modified by Pollard and Siu[4]), the locally exact difference scheme (LEDS)[5] and the power difference scheme (PDS) of Patankar.[6]

0271–2091/86/030129–25$12.50

Received 13 May 1985
Revised 10 September 1985

In section 2 the general transport equations are outlined, and their finite-difference counterparts, formulated by using the control-volume approach, are presented. The nature of the influence coefficients and the restrictions imposed upon the convergence of the discretization schemes are also discussed. Section 3 outlines briefly the solution procedure. Section 4 describes the test problems considered and summarizes their computational details. Results are presented in section 5 and are discussed in section 6. Finally, section 7 presents the conclusions derived from the present study.

2. MATHEMATICAL FORMULATION

2.1. *The transport equations*

Fluid-dynamics and heat/mass-transfer problems of engineering interest are modelled by the Navier–Stokes and conservation equations, that can all be cast into the following general form, in Cartesian tensor notation:

$$\frac{\partial}{\partial t}(\rho\Phi) + \frac{\partial}{\partial x_i}(\rho u_i \Phi) = \frac{\partial}{\partial x_i}\left(\Gamma_\Phi \frac{\partial \Phi}{\partial x_i}\right) + S_\Phi, \tag{1}$$

where i stands for the 3 directions of space, and the summation convention is implied; Φ denotes the variable of interest and Γ_Φ and S_Φ are the diffusion coefficient and source/sink terms, respectively. Furthermore the mass flow rate appearing in (1) must satisfy the continuity equation for the flow field, represented by

$$\frac{\partial \rho}{\partial t} + \frac{\partial}{\partial x_i}(\rho u_i) = 0. \tag{2}$$

For steady-state problems the transient term of equations (1) and (2) is, of course, zero.

2.2. *Finite-difference approximations*

For a uniform grid of length Δx, a simple central difference approximation for the diffusion term is

$$\left(\frac{\partial^2 \Phi}{\partial x^2}\right)_P = \frac{\Phi_E - 2\Phi_P + \Phi_W}{\Delta x^2}, \tag{3}$$

which is, in general, a good approximation, since it is 'third order'.[11] Therefore, the diffusion term presents no particular problem in approximating it. However, convection, which is by its nature a non-symmetrical process, introduces the well-known problem of 'false diffusion' when it is approximated by numerical techniques.[6,7,12,13] In the present contribution we examine eight distinct approximations to the convection term to evaluate their accuracy and practicality for implementation.

In what follows, the subscripts refer to grid nodes around the finite-volume cell of Figure 1. The schemes are as follows, where P_w represents the mesh Peclet number:

(i) The central difference scheme (CDS):

$$\Phi_w = \frac{\Phi_P + \Phi_W}{2}. \tag{4}$$

(ii) The upwind difference scheme (UDS):

$P_w > 0$:

$$\Phi_w = \Phi_W, \tag{5}$$

$P_w < 0$:

$$\Phi_w = \Phi_P.$$

(iii) the hybrid difference scheme (HDS):

$P_w > 2$:

$$\Phi_w = \Phi_W, \tag{6}$$

$P_w < 2$:

$$\Phi_w = \frac{\Phi_P + \Phi_W}{2}.$$

(iv) The quadratic upstream difference scheme (QUDS):

$P_w > 0$:

$$\Phi_w = \frac{\Phi_W + \Phi_P}{2} - \frac{\Phi_{WW} + \Phi_P - 2\Phi_W}{8}, \tag{7}$$

$P_w < 0$:

$$\Phi_w = \frac{\Phi_W + \Phi_P}{2} - \frac{\Phi_E + \Phi_W - 2\Phi_P}{8}.$$

(v) The quadratic upstream extended difference scheme (QUDSE). Equation (7) is modified so that the negative parts of the influence coefficients are incorporated in the source term (for further details see Reference 4):

(8)

(vi) The quadratic upstream extended revised difference scheme (QUDSER). A further modification of the source term is introduced, namely it is linearized using the following conventional form:

$$S(\Phi^*, a) = S(\Phi, a) + S(\Phi, b)\Phi^* : S(\Phi^*, b) = 0, \tag{9}$$

where Φ^* is the current in-store value of Φ (for further details see Reference 4).

(vii) The locally exact difference scheme (LEDS):

$$\Phi_w = \Phi_W + \frac{\exp(P_w/L) - 1}{\exp(P) - 1}(\Phi_P - \Phi_W), \tag{10}$$

where P is the Peclet number.

(viii) The power difference scheme (PDS). Here the exponential function is approximated by a fifth-order power law, and this switches from one expression to another depending on the mesh Peclet number. That is for mesh Peclet numbers (Pe) greater than 10 in magnitude, the power law scheme reverts to the upwind scheme; otherwise an approximation of the form $(1 + \beta)\Phi_U - \beta\Phi_D$ is used where Φ_U and Φ_D are the upwind and downwind nodal values, respectively, and

$$\beta = (1 - 0{\cdot}1|Pe|)^5/|Pe|. \tag{11}$$

This practice results in a fairly accurate scheme in one-dimensional convection-diffusion equations;[7] for further details see Reference 6.

It should be mentioned that the three properties that any successful scheme must possess are that it must be (a) conservative, (b) unconditionally convergent and (c) non-dissipative. None of the existing schemes satisfies all three properties, and their characteristics are discussed in the next section.

2.3. *Method of formulation and influence coefficients*

The general equations in the form of equation (1) are integrated, with appropriate boundary conditions, over the finite control volumes that overlay the domain of interest (Figure 1).

The grid is staggered so that the velocities are located at the cell-faces, where they are required for mass flow-rate evaluations, and the scalar variables are located at the nodal points. Integration

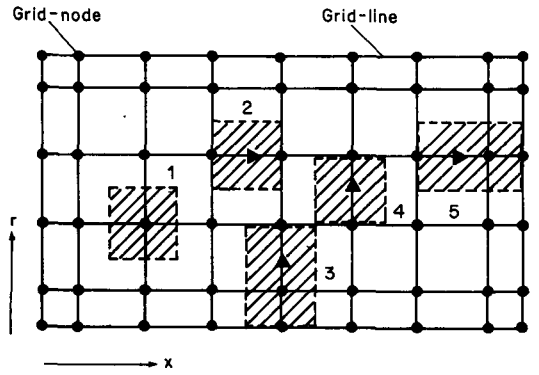

Number	1	2	3	4	5
Control volume type	ϕ and continuity	U	V boundary	V	U boundary

CONTROL VOLUME SPECIFICATION

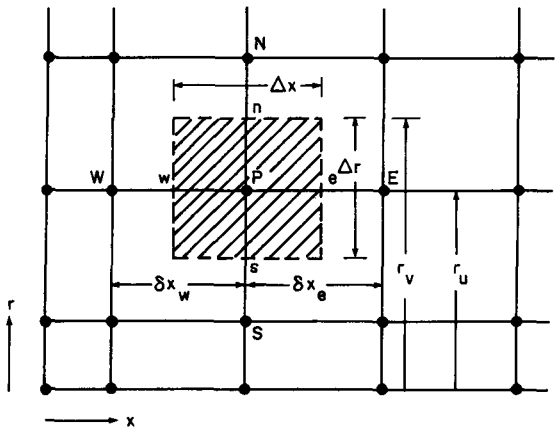

CONTROL VOLUME FOR SCALAR VARIABLE

Figure 1. Control volume and notation

over each cell-face for the control volume shown in Figure 1, using the conventional notation of Patankar,[6] yields the following expressions for the fluxes:

$$J_w^e = \pm\left(r\rho u\Phi - r\Gamma_\Phi \frac{\partial\Phi}{\partial x}\right)_w^e \tag{12}$$

and

$$J_s^n = \pm\left(r\rho v\Phi - r\Gamma_\Phi \frac{\partial\Phi}{\partial r}\right)_s^n,$$

which, when combined for conservation over the single control volume (Figure 1), yield

$$\left(r\rho u\Phi - r\Gamma_\Phi \frac{\partial\Phi}{\partial x}\right)_e A_e^\Phi + \left(r\rho v\Phi - r\Gamma_\Phi \frac{\partial\Phi}{\partial r}\right)_n A_n^\Phi - \left(r\rho u\Phi - r\Gamma_\Phi \frac{\partial\Phi}{\partial x}\right)_w A_w^\Phi - \left(r\rho v\Phi - r\Gamma_\Phi \frac{\partial\Phi}{\partial r}\right)_s A_s^\Phi = rS_\Phi A_P^\Phi. \tag{13}$$

This is the finite-difference representation for the general convection-diffusion equation (1). The As in (13) are the cell face areas as shown in Figure 1. Furthermore, since the common practice of approximating the diffusion terms via the central-difference approximation is satisfactory, no further attention is required for these terms. Attention is directed to the convection terms in equation (13) (e.g. $r\rho u\Phi$ and $r\rho v\Phi$) since it is these approximations which induce false diffusion. The introduction of the approximations made in section 2.2 (i.e. expressions (3)–(11)) will now be discussed.

Substitution of the various convection derivatives (i.e. expressions (4)–(11)) and the diffusion derivative (expression (3)) in equation (13) leads to the final discretized equation for momentum, which has the form:

$$\Phi_P(B_P^\Phi - S(\Phi, b)) = B_E^\Phi\Phi_E + B_W^\Phi\Phi_W + B_N^\Phi\Phi_N + B_S^\Phi\Phi_S + S(\Phi, a), \tag{14}$$

where the linearized form of the source[6] is represented by

$$S_\Phi^* = S(\Phi, a) + S(\Phi, b)\Phi_P. \tag{15}$$

On defining the mesh Peclet number by

$$P_i = C_i/D_i = \rho u_i \Delta x/\Gamma_\Phi,$$

where

$$C_i = \rho u_i; \quad D_i = \Gamma_\Phi/\Delta x,$$

one can describe the various scheme (e.g. the influence coefficients B) in a manner that allows for easy programming in general computer codes, as follows, where $[c_1, c_2]$ denotes the maximum of c_1, c_2.

(i) CDS: conservative and conditionally bounded.

$$B(\mathrm{N}, \mathrm{E}) = D(\mathrm{n}, \mathrm{e}) - \mathrm{mod}(C(\mathrm{n}, \mathrm{e}))/2 + [-C(\mathrm{n}, \mathrm{e}), 0],$$
$$B(\mathrm{S}, \mathrm{W}) = D(\mathrm{s}, \mathrm{w}) - \mathrm{mod}(C(\mathrm{s}, \mathrm{w}))/2 + [C(\mathrm{s}, \mathrm{w}), 0]. \tag{16}$$

Here

$$D_*^\Phi = r_*^\Phi \Gamma_{\Phi,*} A_*^\Phi/\delta x_* \quad \text{and} \quad C_*^\Phi = r_*^\Phi \rho_* u_* A_*^\Phi,$$

where $_*$ stands for (e, w, n, s) and r is the radius.

(ii) UDS: fully conservative and unconditionally bounded.

$$
\begin{aligned}
B(\mathrm{N},\mathrm{E}) &= [D(\mathrm{n},\mathrm{e}), D(\mathrm{n},\mathrm{e}) - C(\mathrm{n},\mathrm{e})],\\
B(\mathrm{S},\mathrm{W}) &= [D(\mathrm{s},\mathrm{w}), D(\mathrm{s},\mathrm{w}) + C(\mathrm{s},\mathrm{w})],\\
S(u,a) &= r_u \Delta r (P_\mathrm{P} - P_\mathrm{E}) : S(u,b) = 0,\\
S(v,a) &= r_v \Delta x (P_\mathrm{P} - P_\mathrm{N}) : S(v,b) = -\Gamma_{\Phi,\mathrm{P}} \Delta x; \quad \text{cylindrical co-ordinates,}\\
&\qquad\qquad = 0 \qquad\qquad \text{cartesian co-ordinates.}
\end{aligned}
\tag{17}
$$

(iii) HDS: fully conservative and unconditionally bounded.

$$
\begin{aligned}
B(\mathrm{N},\mathrm{E}) &= [0, D(\mathrm{n},\mathrm{e}) - C(\mathrm{n},\mathrm{e})/2, -C(\mathrm{n},\mathrm{e})],\\
B(\mathrm{S},\mathrm{W}) &= [0, D(\mathrm{s},\mathrm{w}) + C(\mathrm{s},\mathrm{w})/2, C(\mathrm{s},\mathrm{w})],\\
S(u,a) &= r_u \Delta r (P_\mathrm{P} - P_\mathrm{E}) : S(u,b) = 0,\\
S(v,a) &= r_v \Delta x (P_\mathrm{P} - P_\mathrm{N}) : S(v,b) = -\Gamma_{\Phi,\mathrm{P}} \Delta x \quad \text{cylindrical co-ordinates,}\\
&\qquad\qquad = 0 \qquad\qquad \text{cartesian co-ordinates.}
\end{aligned}
\tag{18}
$$

(iv) QUDS: conservative; boundedness not assured.

$$
\begin{aligned}
B(\mathrm{N},\mathrm{E}) &= M_{(\mathrm{n},\mathrm{e})+}(D(\mathrm{n},\mathrm{e}) - 3C(\mathrm{n},\mathrm{e})/8) + M_{(\mathrm{n},\mathrm{e})-}(D(\mathrm{n},\mathrm{e}) - 3C(\mathrm{n},\mathrm{e})/4 - C(\mathrm{s},\mathrm{w})/8),\\
B(\mathrm{S},\mathrm{W}) &= M_{(\mathrm{s},\mathrm{w})-}(D(\mathrm{s},\mathrm{w}) + 3C(\mathrm{s},\mathrm{w})/8) + M_{(\mathrm{s},\mathrm{w})+}(D(\mathrm{s},\mathrm{w}) + 3C(\mathrm{s},\mathrm{w})/4 + C(\mathrm{n},\mathrm{e})/8),\\
S(u,a) &= r_u \Delta r (P_\mathrm{P} - P_\mathrm{E}) - (M_{\mathrm{w}+} C_\mathrm{w} U_{\mathrm{WW}} + M_{\mathrm{s}+} C_\mathrm{s} U_{\mathrm{SS}} - M_{\mathrm{e}-} C_\mathrm{e} U_{\mathrm{EE}} - M_{\mathrm{n}-} C_\mathrm{n} U_{\mathrm{NN}})/8,\\
S(u,b) &= (M_{\mathrm{e}+} C_\mathrm{e} + M_{\mathrm{n}+} C_\mathrm{n} - M_{\mathrm{w}-} C_\mathrm{w} - M_{\mathrm{s}-} C_\mathrm{s})/8
\end{aligned}
\tag{19}
$$

where

$$M_{j+} = (C_j + \mathrm{mod}(C_j))/(2C_j), \quad j = \mathrm{e}, \mathrm{w}, \mathrm{n}, \mathrm{s}$$

and

$$M_{j-} = (C_j - \mathrm{mod}(C_j))/(2C_j), \quad j = \mathrm{e}, \mathrm{w}, \mathrm{n}, \mathrm{s}.$$

(v) QUDSE: conservatism and boundedness not assured.

$$
\begin{aligned}
B(\mathrm{N},\mathrm{E}) &= [D(\mathrm{n},\mathrm{e}) + 3C(\mathrm{n},\mathrm{e})/4, D(\mathrm{n},\mathrm{e}) - 3C(\mathrm{n},\mathrm{e})/4 - C(\mathrm{s},\mathrm{w})/8,\\
&\qquad D(\mathrm{n},\mathrm{e}) - 3C(\mathrm{n},\mathrm{e})/4, D(\mathrm{n},\mathrm{e}) + 3C(\mathrm{n},\mathrm{e})/4 - C(\mathrm{s},\mathrm{w})/8],\\
B(\mathrm{S},\mathrm{W}) &= [D(\mathrm{s},\mathrm{w}) - 3C(\mathrm{s},\mathrm{w})/4, D(\mathrm{s},\mathrm{w}) + 3C(\mathrm{s},\mathrm{w})/4 + C(\mathrm{n},\mathrm{e})/8,\\
&\qquad D(\mathrm{s},\mathrm{w}) + 3C(\mathrm{s},\mathrm{w})/4, D(\mathrm{s},\mathrm{w}) - 3C(\mathrm{s},\mathrm{w})/4 + C(\mathrm{n},\mathrm{e})/8],\\
S(u,a) &= r_u \Delta r (P_\mathrm{P} - P_\mathrm{E}) - (M_{\mathrm{w}+} C_\mathrm{w} U_{\mathrm{WW}} + M_{\mathrm{s}+} C_\mathrm{s} U_{\mathrm{SS}} - M_{\mathrm{e}-} C_\mathrm{e} U_{\mathrm{EE}} - M_{\mathrm{n}-} C_\mathrm{n} U_{\mathrm{NN}})/8\\
&\qquad - 9(M_{\mathrm{e}+} C_\mathrm{e} U_\mathrm{E} + M_{\mathrm{n}+} C_\mathrm{n} U_\mathrm{N} - M_{\mathrm{w}-} C_\mathrm{w} U_\mathrm{W} - M_{\mathrm{s}-} C_\mathrm{s} U_\mathrm{S})/8,\\
S(u,b) &= (M_{\mathrm{e}+} C_\mathrm{e} + M_{\mathrm{n}+} C_\mathrm{n} - M_{\mathrm{w}-} C_\mathrm{w} - M_{\mathrm{s}-} C_\mathrm{s})/8\\
&\qquad + 9(M_{\mathrm{s}+} C_\mathrm{s} + M_{\mathrm{w}+} C_\mathrm{w} - M_{\mathrm{e}-} C_\mathrm{e} - M_{\mathrm{n}-} C_\mathrm{n})/8,\\
S(v,a) &= r_v \Delta r (P_\mathrm{P} - P_\mathrm{N}) - (M_{\mathrm{w}+} C_\mathrm{w} V_{\mathrm{WW}} + M_{\mathrm{s}+} C_\mathrm{s} V_{\mathrm{SS}} - M_{\mathrm{e}-} C_\mathrm{e} V_{\mathrm{EE}} - M_{\mathrm{n}-} C_\mathrm{n} V_{\mathrm{NN}})/8\\
&\qquad - 9(M_{\mathrm{e}+} C_\mathrm{e} V_\mathrm{E} + M_{\mathrm{n}+} C_\mathrm{n} V_\mathrm{N} - M_{\mathrm{w}-} C_\mathrm{w} V_\mathrm{W} - M_{\mathrm{s}-} C_\mathrm{s} V_\mathrm{S})/8\\
S^\mathrm{c}(v,b) &= (M_{\mathrm{e}+} C_\mathrm{e} + M_{\mathrm{n}+} C_\mathrm{n} - M_{\mathrm{w}-} C_\mathrm{w} - M_{\mathrm{s}-} C_\mathrm{s})/8\\
&\qquad + 9(M_{\mathrm{s}+} C_\mathrm{s} + M_{\mathrm{w}+} C_\mathrm{w} + M_{\mathrm{e}-} C_\mathrm{e} - M_{\mathrm{n}-} C_\mathrm{n})/8,\\
S^\mathrm{r}(v,b) &= -\Gamma_{\Phi,\mathrm{P}} \Delta x / V + S^\mathrm{c}(v,b).
\end{aligned}
\tag{20}
$$

(vi) QUDSER: conservative and bounded. Similar coefficients as for the QUDSE but replace the source by

$$S(\Phi^*, a) = S(\Phi, a) + S(\Phi, b)\Phi^*_\mathrm{P} \quad \text{and} \quad S(\Phi^*, b) = 0, \tag{21}$$

where the * denotes values in store.

(vii) LEDS: fully conservative and unconditionally bounded.

$$B(\mathrm{N}, \mathrm{E}) = C(\mathrm{n}, \mathrm{e})/(\exp(C(\mathrm{n}, \mathrm{e})/D(\mathrm{n}, \mathrm{e})) - 1) + [-C(\mathrm{n}, \mathrm{e}), 0],$$
$$B(S, \mathrm{W}) = C(\mathrm{s}, \mathrm{w})/(\exp(C(\mathrm{s}, \mathrm{w})/D(\mathrm{s}, \mathrm{w})) - 1) + [C(\mathrm{s}, \mathrm{w}), 0], \tag{22}$$

and the source terms are similar to those for the UDS.

(viii) PDS: conservative and bounded.

$$B(\mathrm{N}, \mathrm{E}) = D(\mathrm{n}, \mathrm{e})[0, (1\text{-mod}(C(\mathrm{n}, \mathrm{e})/D(\mathrm{n}, \mathrm{e}))/10^5)] + [-C(\mathrm{n}, \mathrm{e}), 0], \tag{23}$$
$$B(\mathrm{S}, \mathrm{W}) = D(\mathrm{s}, \mathrm{w})[0, (1\text{-mod}(C(\mathrm{s}, \mathrm{w})/D(\mathrm{s}, \mathrm{w}))/10^5)] + [C(\mathrm{s}, \mathrm{w}), 0],$$

and the source terms are similar to those for the UDS.

The main points to be observed with reference to expressions (16)–(23), are:

(a) The CDS influence coefficients become negative if $C > 2D$, and this would in turn lead to oscillatory and non-convergent solutions.[6] One way of overcoming this problem is to use finer grids (down to Peclet numbers of 2), but in practice this is not always feasible owing to high costs.

(b) The UDS influence coefficients are always greater than zero, and the scheme predicts physically plausible solutions at all Peclet numbers. However, its accuracy is limited by its first-order discretization error. This necessitates, in many cases, the use of fine grids, which is expensive.

(c) The HDS uses the advantages of both the CDS and UDS, in that is switches to the UDS when the CDS becomes inaccurate or fails. This practice ensures stability and improves accuracy of the pure UDS.

(d) The QUDS of Leonard,[14] may suffer from convergence problems, as can be seen from the expressions involved in (19); that is the coefficients can become negative if the convection effects are strong enough. Furthermore, negative coefficients appear when $B^{\Phi} - S(\Phi, b) < 0$. One way of overcoming the non-convergence of the scheme is by introducing 'problem-dependent pseudo sources', such as those by Han *et al.*,[15] which soon make the scheme complicated. Another, simpler, way is to switch over to the UDS whenever the Peclet number becomes sufficiently large. Both treatments destroy generality, which for practical implementation, is a strong desideratum.

(e) The QUDSE is an extension of the QUDS,[4] which ensures that the B coefficients are always positive, regardless of the magnitude of the convection term; but the source terms may still induce negative coefficients, as clearly shown in expression (14), when $S(\Phi, b) > 0$.

(f) The QUDSER is a further modification of the QUDSE, in that the overall coefficients are made positive. This is achieved by introducing a linear source which depends on the previous iteration field values.

(g) The LEDS, termed the 'smart upwind method', is exact for one-dimensional problems with source.[7] For the two-dimensional situations considered here, the LEDS is applied locally in each of the co-ordinate directions, although modified, and indeed complicated variations of this particular formulation do exist.[16,17]

(h) The PDS is just a variation of the LEDS, in that it uses an approximation for the exponential function in power form.

3. SOLUTION PROCEDURE

3.1. The algorithm

The SIMPLE algorithm of Patankar and Spalding[18] was used in conjunction with the two-dimensional general code called 2/E/FIX of Pun and Spalding.[19]

The SIMPLE algorithm uses the TDMA procedure to solve for the dependent variables. A system of simultaneous algebraic equations on a line in the y-direction is obtained:

$$(B_P^\Phi - S(\Phi, b))\Phi_P = B_S^\Phi \Phi_S + B_N^\Phi \Phi_N + S_u, \tag{24}$$

where the other neighbouring (e.g. east and west) terms are incorporated in S_u (see equation (14)) and are assumed temporarily as known. It is this formulation (24) which allows a line-by-line iteration method. The continuity equation is not directly solved, but is manipulated instead to yield an equation for 'pressure corrections'.

A brief description of the solution procedure is presented below, but the reader is referred to Reference 19 for full details.

1. Guess the pressure field.
2. Solve the momentum equations on the first line for u and v using the TDMA procedure. Obtain velocities, u^* and v^* based on the guessed pressure field.
3. The above velocities do not, in general, satisfy continuity. Substitution in the continuity equation yields the mass error.
4. The pressure-correction equation is solved, having as source term the above mass error.
5. The pressure corrections are applied to correct pressures and velocities, in such a way as to eliminate the continuity errors.
6. Repeat stages 2 to 5 until convergence has been achieved to a preset tolerance.
7. Advance to next line, and repeat stages 2 to 6.
8. Continue until a domain sweep is completed. (A domain sweep consists of visiting every line in the domain).
9. Perform as many sweeps as required for convergence. This leads to a converged solution with a preset tolerance.

The pressure-correction equation is

$$B_P P_P^{cor} = B_E P_E^{cor} + B_W P_W^{cor} + B_N P_N^{cor} + B_S P_S^{cor} + S(P, a), \tag{25a}$$

where the Bs are given by

$$\begin{aligned} B_E &= \rho_e (r_u \Delta r)^2 / (B_P - S(U, b)), \\ B_W &= \rho_w (r_u \Delta r)^2 / (B_P - S(U, b)), \\ B_N &= \rho_n (r_v \Delta x)^2 / (B_P - S(V, b)), \\ B_S &= \rho_s (r_v \Delta x)^2 / (B_P - S(V, b)), \end{aligned} \tag{25b}$$

and

$$S(P, a) = (r\rho U^*)_w (r_u \Delta r) - (r\rho U^*)_e (r_u \Delta r) + (r\rho V^*)_s (r_v \Delta x) - (r\rho V^*)_n (r_v \Delta x), \tag{25c}$$

where $S(P, a)$, is the negative of the discretized continuity equation which has the form

$$(r\rho U)_e A_e - (r\rho U)_w A_w + (r\rho V)_n A_n - (r\rho V)_s A_s = 0. \tag{26}$$

3.2. Boundary conditions

In general, the two types of boundary conditions encountered (Dirichlet and Neumann), are treated as follows:

(i) The boundary conditions are incorporated by modifying the B coefficients in the discretized form of the equations.
(ii) For the QUICK/E/ER, the problem associated with the extra upstream values required was overcome by setting the upstream value equal either to the boundary value or the first internal grid point value. These two practices gave very similar results.

4. THE TEST PROBLEMS CONSIDERED

The schemes were applied to a series of uniform property, 2D laminar flows, two of which are presented here: flow through a sudden enlargement in a pipe and flow in a cavity with a moving lid. These physical situations were chosen mainly because much attention has been focused on them, as they do exhibit well the effects of false diffusion. The schemes were tested over a wide range of Reynolds numbers, between 50 and 2000 and with different numbers of grid nodes, between 100 (10×10) and 1200(30×40). Finally, the schemes were also tested at artificially high Reynolds number (10^4–10^6) 'laminar' flow.

4.1. Flow through a sudden enlargement in a circular pipe

Fluid enters the half-open pipe of Figure 2, of length equal to 25 times the half-open pipe diameter. There is a recirculation region formed behind the closed half of the pipe, within a length l_r from the entrance, and the velocity-vector directions within the eddy are inclined at various angles to the local grid. This makes the solution to this problem (as well as the next) a good test on 'false diffusion'. The boundary conditions are:

Inlet: specified parabolic velocity profile.
Outlet: $\partial u/\partial x = 0$ and $v = 0$.
Wall boundaries: $u = 0$ and $v = 0$.
Axis of symmetry: $\partial u/\partial r = 0$ and $v = 0$.

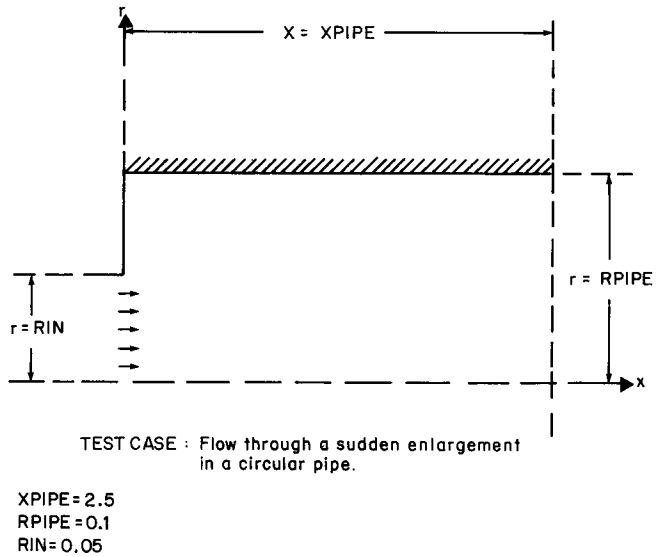

Figure 2. Sudden enlargement

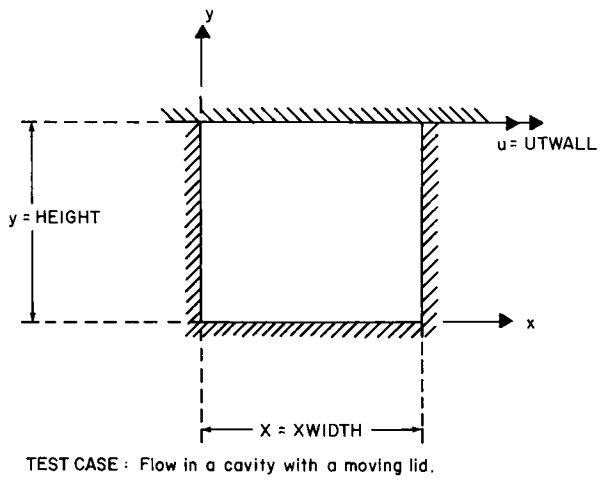

Figure 3. Cavity with moving lid

4.2. *Flow in a cavity with a moving lid*

Fluid is forced to rotate within the square cavity of Figure 3, by a moving lid with specified velocity, U_{top}. The boundary conditions are:

Top wall: $u = U_{top}$ and $v = 0$.

Other walls: $u = 0$ and $v = 0$.

4.3. *Convergence criterion*

The convergence criterion, for both cases, was that no variable changes more than 10^{-6} with iteration, together with the requirement that the sum of the absolute (volume) continuity errors be less than 0·1 per cent of a typical volume flow rate. In general, the latter requirement was satisfied before the former.

5. PRESENTATION OF RESULTS

5.1. *Flow through a sudden enlargement in a circular pipe*

Fluid flowing in a pipe, containing an abrupt change in cross-sectional area, results in fluid flow reversal in the immediate vicinity of the step change. In general the flow reversal is characterized by points of flow detachment and re-attachment, and the location of the re-attachment point is a function of the following quantities:[21]

(i) the size of the enlargement
(ii) the inlet velocity profile
(iii) the inlet Reynolds number.

Recent efforts to produce accurate results for this test case have been reported in References 12–14. Leschziner[22] compared results predicted by three schemes[5,13,14] and reported no difference in the predictions of the re-attachment length.

Experimental results for this test case have been reported in Reference 23 and calculations using the upwind difference scheme have been reported in Reference 24. It was found that the UDS

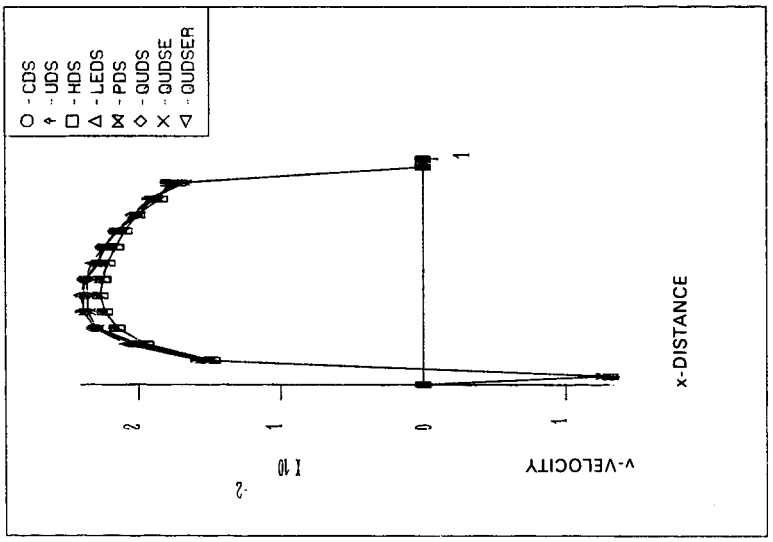

Figure 5. Radial-velocity profile at centre-line for various schemes

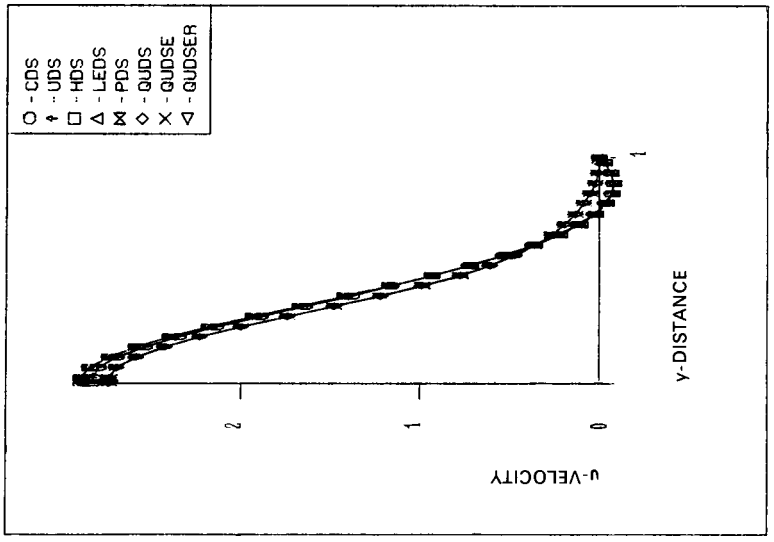

Figure 4. Axial velocity profile at centre-line, for various schemes

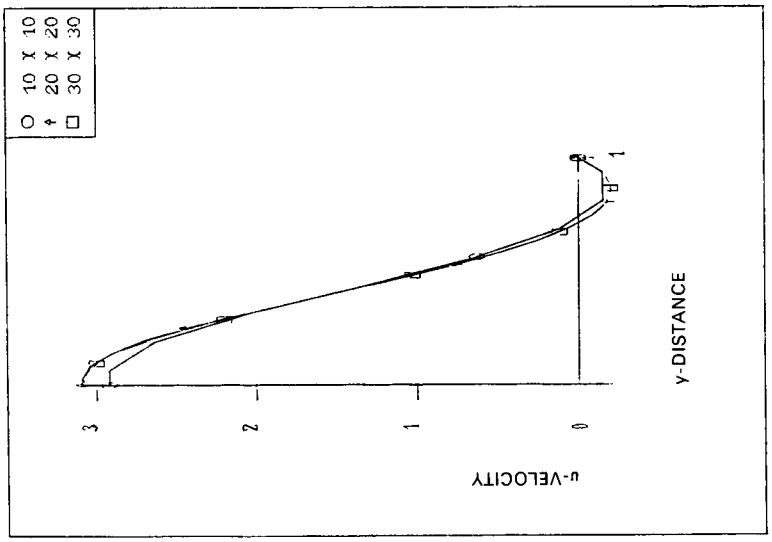

Figure 7. Grid-refinement studies for the QUDS

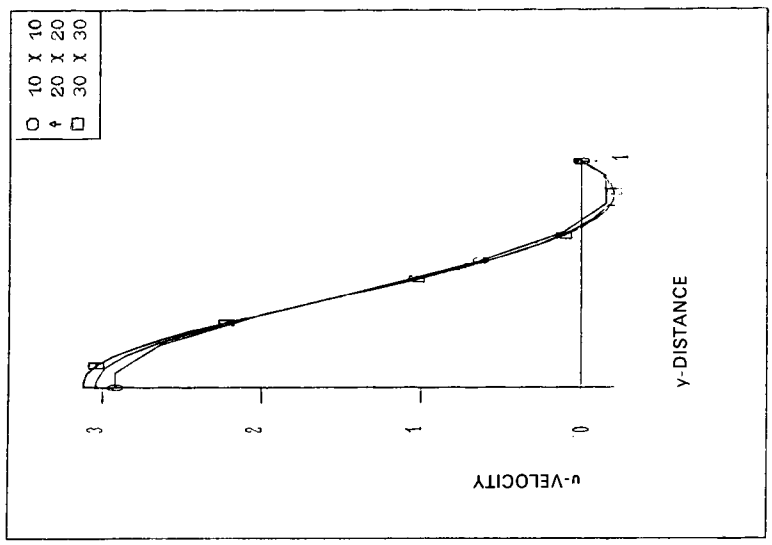

Figure 6. Grid-refinement studies for the CDS

Table I. Computational details to obtain a given accuracy (for $Re = 50$, 100, 150 and 200) using various schemes

Scheme	Reynolds number	N	T	N/N_u	T/T_u	T/N
CDS	50	166	1640	1·506	1·803	9·880
	100	194	1932	1·863	2·247	9·960
	150	194	1966	1·974	2·427	10·113
	200	206	2266	2·016	2·691	11·003
UDS	50	110	900	1·000	1·000	8·273
	100	104	860	1·000	1·000	8·269
	150	98	810	1·000	1·000	8·265
	200	102	842	1·000	1·000	8·255
HDS	50	106	866	0·964	0·952	8·170
	100	102	820	0·981	0·953	8·170
	150	98	980	1·000	0·963	7·959
	200	100	818	0·980	0·965	8·120
LEDS	50	108	924	0·982	1·015	8·556
	100	104	872	1·000	1·013	8·385
	150	100	818	1·020	1·010	8·180
	200	100	850	0·980	1·009	8·500
PDS	50	112	888	1·018	0·976	7·929
	100	108	844	1·038	0·981	7·815
	150	104	786	1·061	0·970	7·558
	200	106	820	1·039	0·974	7·736
QUDS	50	98	1180	0·891	1·296	12·041
	100	96	1110	0·923	1·290	11·563
	150	96	1044	0·980	1·280	10·875
	200	94	1086	0·922	1·289	11·553
QUDSE	50	94	1214	0·855	1·334	12·915
	100	92	1102	0·885	1·281	11·978
	150	92	1016	0·939	1·281	11·043
	200	92	1082	0·902	1·285	11·761
QUDSER	50	154	1958	1·400	2·141	12·649
	100	158	1886	1·519	2·193	11·937
	150	160	1784	1·633	2·202	11·150
	200	158	1852	1·549	2·200	11·722

underestimates both the length and the intensity of the recirculation zone compared to the CDS.

Here attention is directed to the predictions by the various schemes of the re-attachment lengths and of the centre-line velocity profiles, for different Reynolds numbers and grid sizes. Calculations for this test case were performed at $Re = 50$ to 1000 although only results for $Re = 200$ and 300 are presented here, owing to space restrictions. Predictions by using the various schemes for centre-line velocity profiles are shown in Figures 4 and 5, for a grid of 16×24.

For grid independency purposes, results for the axial-velocity profiles at $Re = 200$ and grids of 10×10, 20×20 and 30×30 are depicted in Figure 6 for the CDS, and in Figure 7 for the QUDS. Table I summarizes details of the computational requirements for each of the schemes, with reference to the UDS. In this table, N is the number of iterations required to obtain a given accuracy. T is time in CPU seconds, and N_u, T_u are the N and T for the UDS.

Results for the re-attachment lengths are presented in Figures 8 and 9 for $Re = 50$ to 300.

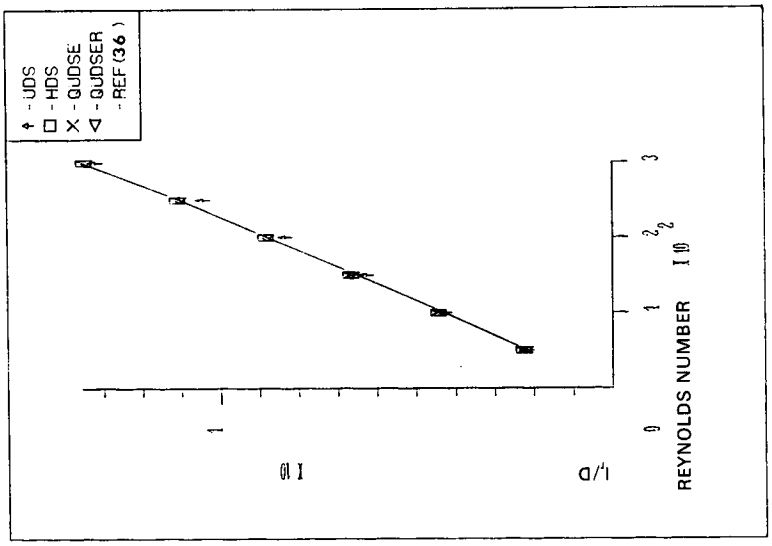

Figure 9. Re-attachment length variation with Reynolds number (l_r/d against Re)

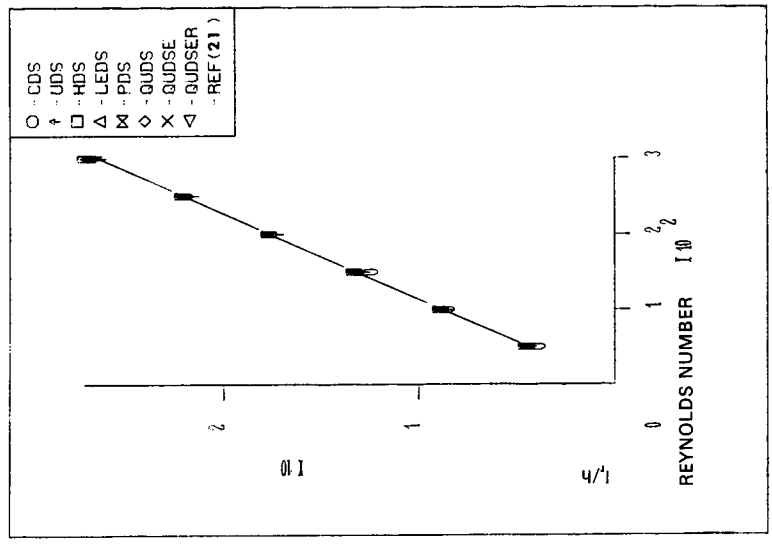

Figure 8. Re-attachment length variation with Reynolds number (l_r/h against Re)

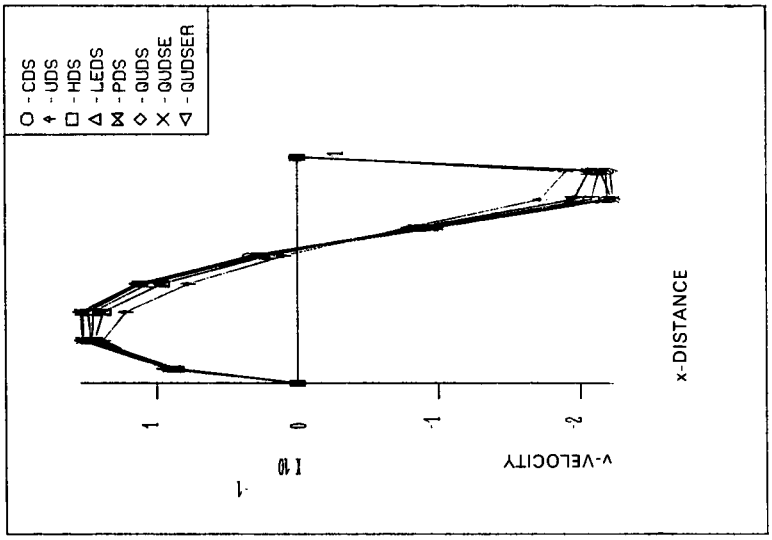

Figure 11. Radial-velocity profile at centre-line for various schemes

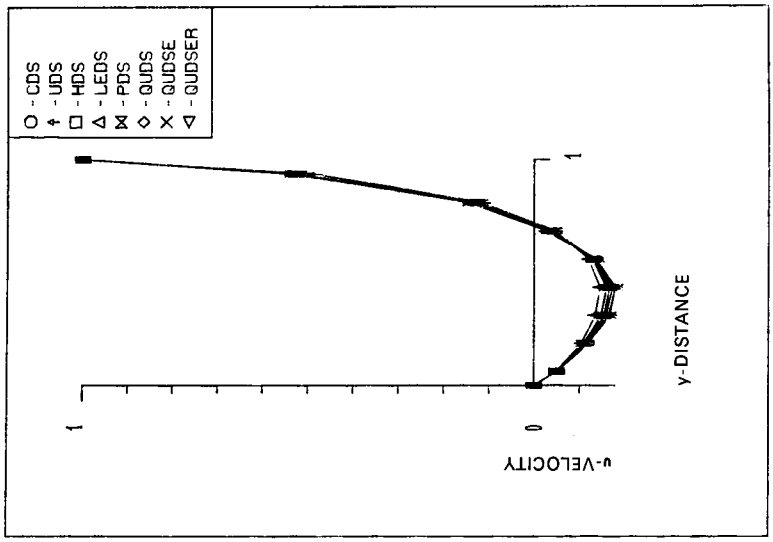

Figure 10. Axial velocity profile at centre-line, for various schemes

Table II. Comparison of re-attachment lengths using various schemes for $Re = 50$, 100, 150 and 200

Scheme	Reynolds number	l_r/h	l_r/D	l_r/hRe
CDS	50	3·95	1·97	0·079
	100	8·10	4·05	0·081
	150	12·51	6·25	0·083
	200	16·66	8·33	0·083
UDS	50	4·38	2·19	0·088
	100	8·59	4·29	0·086
	150	12·84	6·42	0·086
	200	17·29	8·65	0·086
HDS	50	4·52	2·26	0·090
	100	8·91	4·45	0·089
	150	13·33	6·67	0·089
	200	17·68	8·84	0·088
LEDS	50	4·52	2·26	0·090
	100	8·90	4·45	0·089
	150	13·32	6·66	0·089
	200	17·68	8·84	0·088
PDS	50	4·52	2·26	0·090
	100	8·90	4·45	0·089
	150	13·32	6·66	0·089
	200	17·67	8·84	0·088
QUDS	50	4·46	2·23	0·089
	100	8·88	4·44	0·089
	150	13·26	6·63	0·088
	200	17·64	8·82	0·088
QUDSE	50	4·46	2·23	0·089
	100	8·86	4·43	0·089
	150	13·30	6·65	0·089
	200	17·64	8·82	0·088
QUDSER	50	4·46	2·22	0·089
	100	8·86	4·43	0·089
	150	13·30	6·65	0·089
	200	17·64	8·82	0·088

Table III. Reference re-attachment lengths used for comparison[21,36]

Reynolds number	Reference 21 l_r/h	Reference 36 l_r/D	Reference 21 l_r/hRe
50	4·41	2·2	0·0882
100	8·81	4·3	0·0881
150	13·22	6·5	0·0881
200	17·62	8·8	0·0881

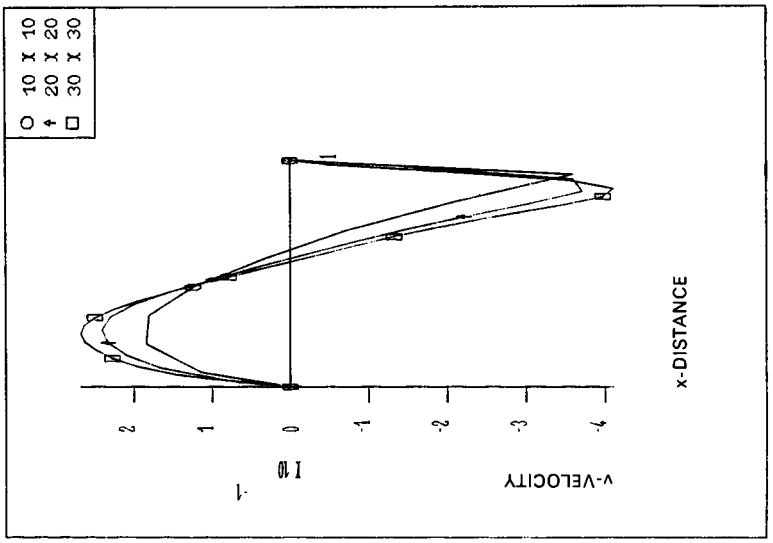

Figure 13. Grid-refinement, radial velocity for the CDS

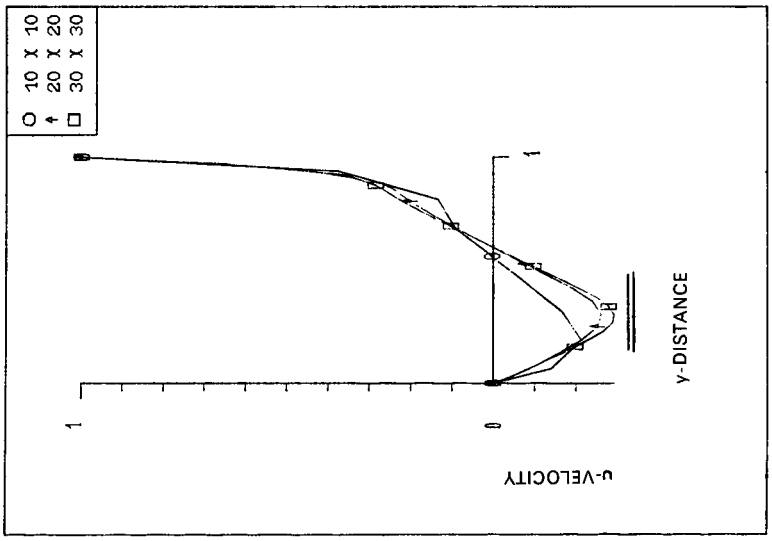

Figure 12. Grid-refinement, axial velocity for the CDS

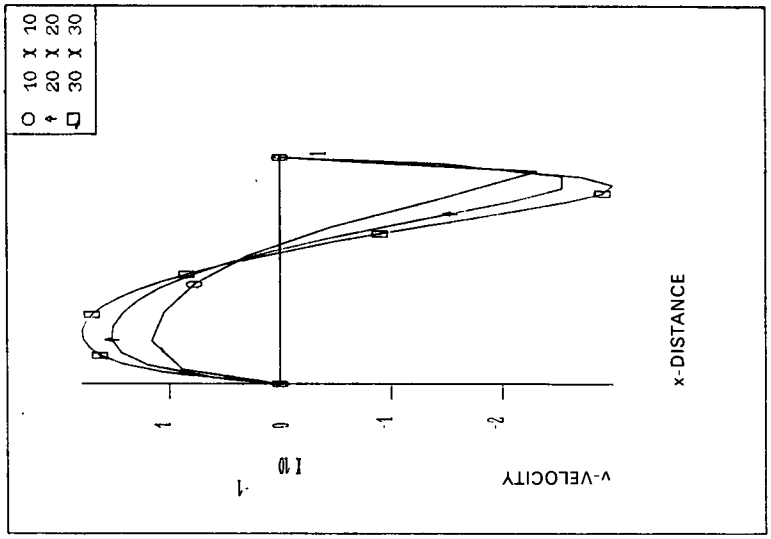

Figure 15. Grid-refinement, radial velocity for the UDS

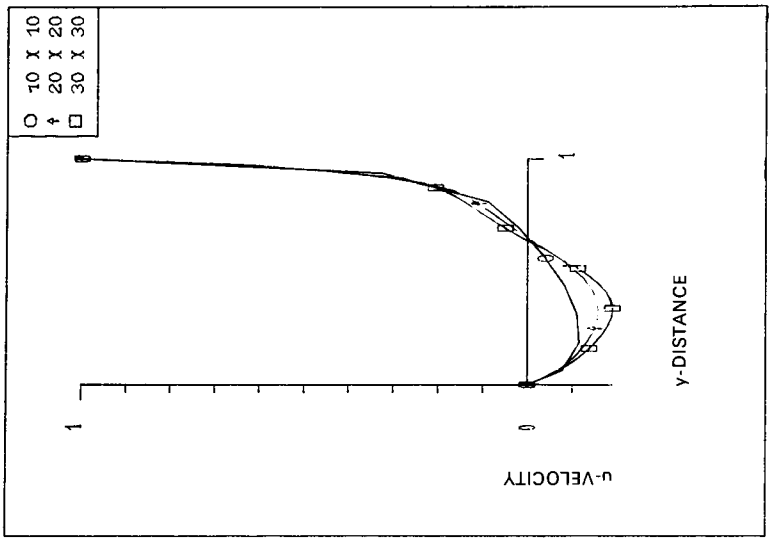

Figure 14. Grid-refinement, axial velocity for the UDS

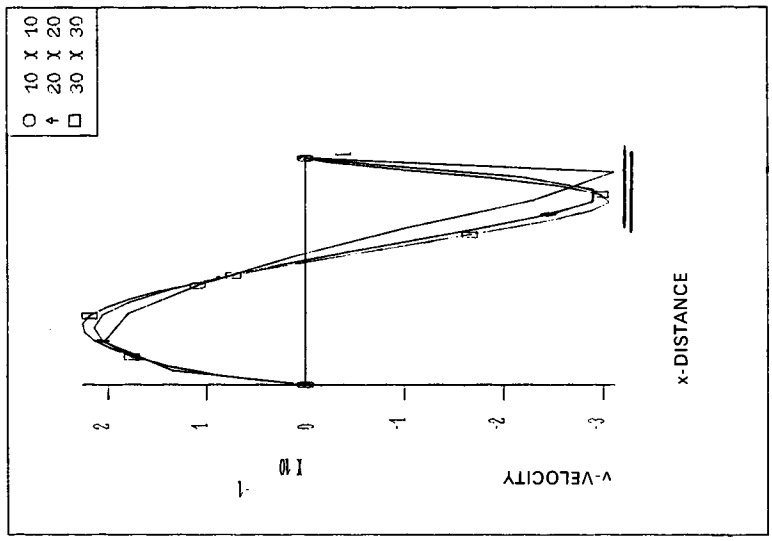

Figure 17. Grid-refinement, radial velocity for the QUDS

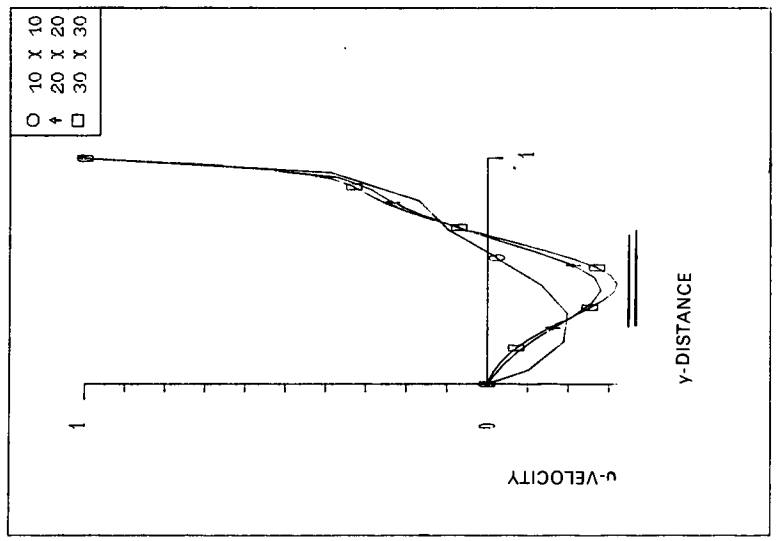

Figure 16. Grid-refinement, axial velocity for the QUDS

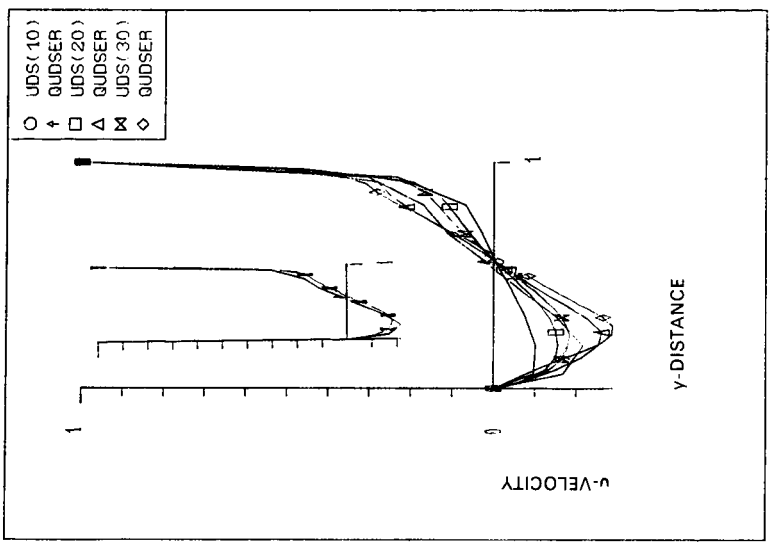

Figure 18. Grid-refinement, axial velocity for the UDS/QUDSER ($Re = 1000$)

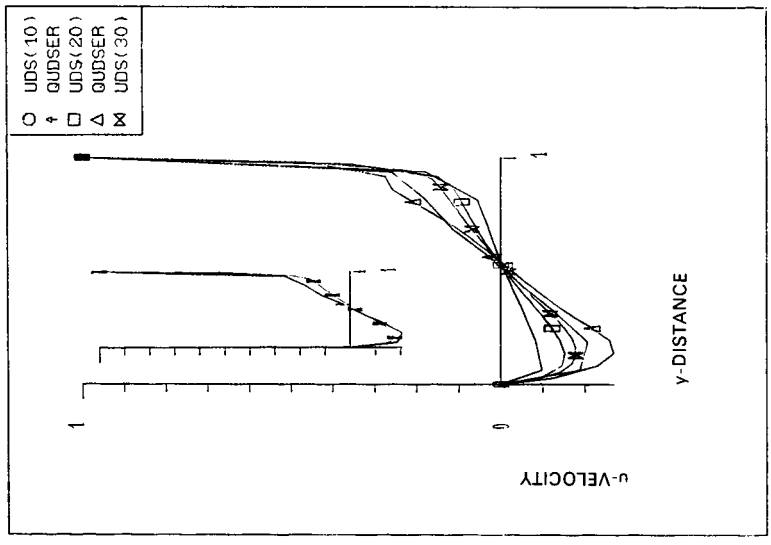

Figure 19. Grid-refinement, axial velocity for the UDS/QUDSER ($Re = 2000$)

Table II lists the normalized re-attachment lengths obtained for a 16 × 24 grid for various Reynolds numbers, and Table III the values given in References 21 and 36.

5.2. *Flow in a cavity with a moving lid*

Steady-state flow in a square cavity is a popular problem for testing and comparing numerical methods, owing to its geometric simplicity and highly elliptic nature. However, most of the earlier work[25–31] dealt with the stream-function–vorticity formulation. Burggraf[25] has performed an excellent study of this test case, for a range of successively finer grids, and various high Reynolds numbers, using the CDS, for the convective term. Recently, much work has been devoted to this test case, and numerous publications have appeared, but an extensive review is beyond the scope of the present work. However, readers are referred to the excellent review papers by De Vahl Davis and Mallinson,[29] Tuann and Olson[32] and Bozeman and Dalton.[33] Although the present study considers the lid velocity to be constant, examples for space-varying lid velocities have also been reported.[34]

Calculations were performed for $Re = 100$ and 400, with a grid set-up of 10 × 10. Results for the centre-line velocity profiles for $Re = 100$ are presented in Figures 10 and 11. For grid-independency purposes, solutions for grids of 20 × 20 and 30 × 30 were also computed, at $Re = 100$ to 2000. Results for the centre-line velocity profiles, for these studies, are depicted in Figures 12 and 13 for the CDS, Figures 14 and 15 for the UDS and Figures 16 and 17 for the QUDS, for $Re = 400$. Where indicated, a reference band is depicted as reported in Reference 4. Finally, Figures 18 and 19 depict the centre-line u-velocity profiles for the UDS/QUDSER schemes at $Re = 1000$ and 2000, respectively. Table IV shows the details for the computational requirements for each of the schemes, with reference to the UDS.

Table IV. Computational details to obtain a given accuracy using various schemes for $Re = 100$ and 400

Scheme	Reynolds number	N	T	N/N_u	T/T_u	T/N
CDS	100	126	24	1·518	2·000	0·191
	400	191	56	2·274	4·308	0·293
UDS	100	83	12	1	1	0·143
	400	84	13	1	1	0·155
HDS	100	79	11	0·952	0·917	0·139
	400	87	12	1·036	0·923	0·138
LEDS	100	90	15	1·084	1·250	0·167
	400	89	15	1·060	1·154	0·169
PDS	100	87	13	1·048	1·048	0·149
	400	88	14	1·048	1·077	0·159
QUDS	100	91	18	1·096	1·500	0·198
	400	101	19	1·202	1·462	0·188
QUDSE	100	295	96	3·554	8·000	0·325
	400	277	84	3·298	6·462	0·303
QUDSER	100	185	48	2·229	4·003	0·259
	400	200	43	2·381	3·308	0·215

6. DISCUSSION OF RESULTS

6.1. *Flow through a sudden enlargement in a circular pipe*

The u-velocity profiles (Figure 4) fall into two groups (i.e. as predicted by first- and second-order methods) whereas the v-velocity profiles fall into three groups (i.e. CDS/QUDS, QUDSE/R and UDS/HDS/LEDS/PDS).

The second-order methods (namely CDS/QUDS/E/R) predicted similar, and in some instances identical, velocity profiles which were always at lower values, as compared to the first-order methods. This may be attributed to the larger discretization error of the latter.

Although different software writers adopt different techniques and, therefore, computer times for the various formulations are of low importance in absolute terms, it is still of relative interest to examine Table I. This examination reveals the following findings, relative to the UDS, for Reynolds numbers 50, 100, 150 and 200.

The CDS requires about 24 per cent more computational time per node with an increase of 78 per cent in the number of iterations, whereas the QUDS requires 40 per cent more computational time per node with a decrease of 7 per cent in the number of iterations. This clearly shows an advantage in having a higher order interpolant (i.e. decrease in iteration numbers), the disadvantage being that there is an increase in the unit computational time. The HDS/LEDS and PDS were all similar in their requirements, which suggests that the LEDS does perform well, given the fact that exponential functions have to be evaluated. For the QUDSER the time per iteration was 40 per cent more than for the UDS, with an increase of 52 per cent in the number of iterations required. The QUDSE was similar to the QUDSER in unit time, but required fewer iterations by a factor of 1·7.

Grid independency studies (Figures 6 and 7 for the CDS and QUDS, respectively, at $Re = 200$) clearly show that the CDS velocity profiles are still grid dependent even for a grid size of 30×30, whereas the QUDS gives virtually grid independent results for the 20×20 and 30×30 grid sizes. It is worth noting that the 10×10 velocity profiles predicted by the CDS and QUDS were identical.

The re-attachment length, an important feature of this test case, is tabulated in Table II, together with results obtained from other sources in Table III. Predictions have been obtained over a range of Reynolds numbers from 50 to 1000. The results for the re-attachment lengths of Table II were in good agreement with those in Table III. The predicted re-attachment lengths are plotted in Figures 8 and 9, where Figure 8 shows l_r/h against Re, and Figure 9 shows l_r/d against Re.

For low Reynolds number flows ($\leqslant 300$), the re-attachment length data indicate a linear relationship with respect to the Reynolds number,[36–38] as demonstrated by Figures 8 and 9. The results confirm the findings of Leschziner,[22] and are in close agreement for all schemes.

6.2. *Flow in a cavity with a moving lid.*

The velocity profiles, depicted in Figures 10 and 11, are all in close agreement except for the UDS profiles, which are all always underpredicted (e.g. flatter profiles).

An examination of Table IV reveals the following findings, relative to the UDS, for Reynolds numbers 100 and 500. The first-order schemes were all found to be similar in their computational requirements per iteration except for the LEDS which was slightly higher in its requirements. The QUDS required about 30 per cent more computational time per iteration with an increase of 15 per cent in the number of iterations required.

The QUDSE required 60 per cent more computational time per iteration with a 2-fold increase in the number of iterations.

Grid independency studies are depicted in Figures 12 and 13 for CDS, Figures 14 and and 15 for UDS and Figures 16 and 17 for QUDS, at $Re = 400$. Results for $Re = 1000$ and 2000 are depicted in Figures 18 and 19.

The results show that the CDS and QUDS are virtually identical and are grid independent for grids of around 30×30, whereas the UDS predicts a much flatter profile and the solution is still grid dependent for grids of 30×30. For $Re = 1000$ and 2000, the QUDSER predicted results much closer to the true solution, whereas the UDS predicted highly diffused solutions. The QUDSER with a 10×10 grid, predicted results similar to the UDS with 30×30 grid, a fact which is clearly depicted by the inserts in Figures 18 and 19, for the high Reynolds number flows.

7. CONCLUSIONS

A comparative study in terms of accuracy and computer requirements has been performed for eight numerical schemes, which were applied to a series of 2D convection-diffusion problems, two of which were presented. The main findings of this work may be summarized as follows:

1. The CDS/QUDS/E proved the most unstable schemes at high Reynolds numbers.
2. The UDS/HDS/LEDS/PDS/QUDSER suffered from no instabilities for the test cases considered here.
3. The performances of the QUDS/E/R were found to be accurate and identical for QUDSE/R, when they converged, for all Reynolds numbers considered.
4. The QUDS/E were found to be unstable for high flow rates/coarse grids, unlike the QUDSER which was stable for those flows considered.
5. The QUDSER was the most expensive scheme in terms of computational requirements; the reason being that the source terms are less implicit in nature than the QUDSE.
6. In general the QUDSER required twice the number of iterations to secure the same level of accuracy as the QUDSE scheme. It is felt that, although the computational requirements are clearly also a function of the particular programming technique, they still indicate that the QUDSER is, relatively, the most expensive scheme.
7. Modifications to the sources of QUDSER proved less fruitful (i.e. when $S_P < 0$ then no source linearization is required). The above statement is therefore valid, independently of the way the source is linearized.
8. The QUDSE/R required more iterations than any other scheme, apart from the QUDSER, to secure convergence for flow situations with recirculating zones.
9. The QUDSER predicted highly accurate solutions for coarser grids, unlike the UDS which even for a three fold increase in grid fineness, in each grid direction, predicted results slightly worse than the QUDSER.
10. The UDS/HDS requires a many-fold increase in the grid fineness to obtain accuracies close to the QUDS/E/R schemes.
11. In terms of accuracy and computational efficiency it appears that the QUDS/E/R may offer the best compromise. Unfortunately, none of these schemes are satisfactory from all aspects. Thus, they may be unstable (or non-convergent) for high flow rates/coarse grids. Furthermore, divergence was also encountered when the authors applied them to some complex engineering situations.[40] It is the authors' opinion that their accuracy is of limited importance if their range of applicability is small. They can be recommended for carefully controlled cases of 'academic' interest.
12. The unconditionally convergent schemes (UDS/HDS/LEDS/PDS) can be significantly inaccurate for coarse grids, in such cases as the square cavity with the moving lid; and they

may require considerable grid refinement to produce acceptably accurate results, which makes them expensive. This may not be a severe limitation, however, as the efficiency of computer hardware and software increases rapidly. Furthermore, their simplicity and generality of application is still attractive for complex engineering applications, where errors associated with physical uncertainties and the related modelling (i.e. turbulence, turbulence–chemistry interactions, two-phase processes, etc.) are, in general, likely to be more predominant than discretization and false-diffusion errors. One must, of course, be very careful to ensure real grid-independency of the results.

13. The above findings reveal an unsatisfactory situation where the more accurate schemes are not of general applicability, and the more general schemes may be too inaccurate within present practical resources. New directions in research on this topic are needed. The authors have diverted attention from the locally-1D schemes and are experimenting with flow-directed schemes. The findings of this work will be reported elsewhere.[41]

REFERENCES

1. A. K. Runchal, D. B. Spalding and M. Wolfshtein, 'Numerical solution of the elliptic equations for transport of vorticity, heat, and matter in two-dimensional flow', *High-speed computing in fluid-dynamics. The Physics of Fluids Supplement II*, 1969, pp. 21–28.
2. K. E. Barrett, 'The numerical solution of singular-perturbation boundary-value problems', *Q.J. Mech. Appl. Math.*, **XXVII**, pt. 1 (1974).
3. B. P. Leonard, 'Newsflash: upstream parabolic interpolation', *Proc. of 2nd GAMM conference on Numerical Methods in Fluid Mechanics*, Koln, W. Germany, 1977.
4. A. Pollard and L. W. Alan Siu, 'The calculation of some laminar flows using various discretisation schemes', *Comp. Meth. Appl. Mech. Eng.*, **35**, 293–313 (1982).
5. D. B. Spalding, 'A novel finite difference formulation for differential expressions involving both first and second derivatives', *Int. j. numer. methods eng.*, **4**, 557–559 (1972).
6. S. V. Patankar, *Numerical Heat Transfer*, McGraw-Hill, New York, 1980.
7. M. K. Patel, N. C. Markatos and M. Cross, 'A critical evaluation of seven discretization schemes for convection-diffusion equations', *Int. j. numer. methods fluids*, **5**, 225–244 (1985).
8. D. B. Spalding, 'A general purpose computer program for multi-dimensional one- and two-phase flow', *Mathematics and Computers in Simulation*, North Holland Press, 1981, Vol. XXIII, pp. 267–276.
9. N. C. Markatos, A. Moult, P. J. Phelps and D. B. Spalding, 'The calculation of steady, three-dimensional, two-phase flow and heat transfer in steam generators', *Proc. ICHMT seminar*, Dubrovnik, Yugoslavia, Hemisphere, Washington, 1978, pp. 485–502.
10. N. C. Markatos and D. Kirkcaldy, 'Analysis and computation of three-dimensional, transient flow and combustion through granulated propellants', *Int. J. Heat Mass Transfer*, **26**, (7), 1037–1053 (1983).
11. B. P. Leonard, M. Leschziner and J. McGuirk, 'Third-order finite-difference method for steady two-dimensional convection', *Num. Meths. in Laminar and Turbulent Flow*, 807–819 (1978).
12. G. D. Raithby, 'A critical evaluation of upstream differencing applied to problems involving fluid flow', *Comp. Meth. Appl. Mech. Eng.*, **9**, 75–103 (1976).
13. G. D. Raithby, 'Skew upstream differencing schemes for problems involving fluid flow', *Comp. Meth. Appl. Mech. Eng.*, **9**, 153–164 (1976).
14. B. P. Leonard, 'A stable and accurate convective modelling procedure based on quadratic upstream interpolation', *Comp. Meth. Appl. Mech. Eng.*, **19**, 59–98 (1979).
15. T. Han, J. A. C. Humphrey and B. E. Launder, 'A comparison of hybrid and quadratic-upstream differencing in high Reynolds number elliptic flows', *Comp. Meth. Appl. Mech. Eng.*, **29**, 81–95 (1981).
16. J. C. Chien, 'A general finite-difference formulation with application to Navier–Stokes equations', *Comput. Fluids*, **5**, 15–31 (1977).
17. D. N. De G. Allan and R. V. Southwell, 'Relaxation methods applied to determine the motion in two dimensions of a viscous fluid past a fixed cylinder', *Q. J. Mech. Appl. Math.* **VIII**, Pt. 2, 129 (1955).
18. S. V. Patankar and D. B. Spalding, 'A calculation for heat, mass and momentum transfer in three-dimensional parabolic flows', *Int. J. Heat Mass Transfer*, **15**, 1787–1806 (1972).
19. W. M. Pun and D. B. Spalding, 'A general computer program for two-dimensional elliptic flows', *Report HTS/76/2*, Imperial College, London, 1976.
20. R. K. Shah and A. L. London, 'Laminar flow forced convection in ducts', *Adv. in Heat Transfer Series Supp. 1*, Academic Press, 1978.
21. A. Pollard, 'Entrance and diameter effects on the Laminar flow in sudden expansions', in B. E. Launder and J. A. C.

Humphrey (eds) *Momentum and Heat Transfer Processes in Recirculating flows*, ASME Htd. **13,** 21–26 (1980).
22. M. A. Leschziner, 'Practical evaluation of three finite difference schemes for the computation of steady-state recirculating flows', *Comp. Meth. Appl. Mech. Eng.*, **23,** 293–312 (1980).
23. M. K. Denham and M. A. Patrick, 'Laminar flow over a Downstream facing step in a Two-dimensional flow channel', *Trans. Inst. Chem. Engineers (Britain)*, **52,** 361–367 (1974).
24. D. J. Atkins, S. J. Maskell and M. A. Patrick, 'Numerical Predictions of separated flows', *Int j. numer. methods eng.*, **15,** 129–144 (1980).
25. O. R. Burggraf, 'Analytical and numerical studies of the structure of steady separated flows', *J. Fluid Mech.*, **24,** 113–151 (1966).
26. D. Greenspan, 'Numerical studies of prototype cavity flow problems', *The Computer Journal*, **12,** 89–96 (1969).
27. M. Fortin, R. Peyret and R. Temam, 'Approximations by a study of recirculating flows', *Lecture notes in Physics*, Springer-Verlag, NY, 1971, Vol. 8, pp. 337–342.
28. P. Roache, 'The LAD, NOS and split NOS methods for the steady-state Navier–Stokes equations', *Comput. Fluids*, **3,** 179–195 (1975).
29. G. De Vahl Davis and G. D. Mallinson, 'An evaluation of upwind and central difference approximations by study of recirculating flows', *Comput. Fluids*, **4,** 29–43 (1976).
30. S. G. Rubin and P. K. Khosla, 'Polynomial Interpolation methods for viscous flow calculations', *J. Comput. Phys.*, **24,** 217–244 (1977).
31. M. M. Gupta and R. P. Manohar, 'Boundary approximations and accuracy', *J. Comput. Phys. in Viscous Flow Computations*, **31,** 265–288 (1979).
32. S. Y. Tuann and M. D. Olson, 'Review of computing methods for recirculating flows', *J. Comput. Phys.*, **29,** 1–19 (1978).
33. J. D. Bozman and C. Dalton, 'Numerical study of viscous flow in a cavity', *J. Comput. Phys.*, **12,** 348 (1973).
34. M. Bourcier and C. Francois 'Integration numeric de equation de navier stokes un Domaine Karre', *Rech. Aeosp.*, No. 131, 23–33 (1969).
35. Wei, Shyy, 'Determination of relaxation factors for high cell Peclet number flow simulation', *Comp. Meth. Appl. Mech. Eng.*, **43,** 221–230 (1984).
36. E. O. Macagno and T. K. Hung, 'Computational and experimental study of a captive annular eddy', *J. Fluid Mech.*, **28,** 43–64 (1967).
37. L. H. Back and E. J. Roschke, 'Shear-layer flow regimes and wave instabilities and re-attachment lengths downstream of an abrupt circular channal expansion', *J. Appl. Mech. Trans. ASME. Series E.*, **39,** 677 (1972).
38. A. Iribarne, F. Frantisak, R. L. Hummel and J. W. Smith, 'An experimented study of instabilities and other flow properties of a laminar pipe jet', *AICHE. J.*, **18,**(4), 689 (1972).
39. T. K. Bhattacharyya and A. B. Datta 'A residual method of finite differencing for the elliptic transport problem and its applications to cavity flow', *Int. j. numer. methods fluids*, **5,** 71–80 (1985).
40. N. C. Markatos and M. K. Patel 'Ten discretisation schemes applied to fire modelling', *Appl. Math. Modelling*, to be published, (1986).
41. M. K. Patel, N. C. Markatos and M. Cross, 'Method of reducing false-diffusion errors in convection-diffusion problems', *Appl. Math. Modelling*, **9,** 302–306 (1985).